ELSEVIER

Succession in mixed boreal forest of Russia: Markov models and non-Markov effects

Vladimir N. Korotkov [a], Dmitrii O. Logofet [b,*], Michel Loreau [c]

[a] *Department of Forestry Informatization, All-Russia Research Information Center for Forest Recources, Novocheremushkinskaya Street 69, Moscow 117418, Russia*
[b] *Laboratory of Mathematical Ecology, Institute of Atmospheric Physics RAS, Pyzhevsky Lane 3, Moscow 109017, Russia*
[c] *Laboratoire d'Ecologie, Ecole Normale Supérieure, UMR 7625, 46 rue d'Ulm, F-75230 Paris Cedex 05, France*

Abstract

An aggregated scheme is presented for the ideal course of the post-tillage succession (natural overgrowing) among 15 forest types in a mixed (coniferous-broad-leaved) forest in Central Russia. A first, traditional Markov chain model describes the course of succession leading eventually to the climax state, which is recognised to be a polydominant spruce-broad-leaved forest. The model predicts the average times it would take to reach the climax from any other stage of succession, while the current state of the forest is estimated by means of a GIS technology. Present geobotanic knowledge, however, assures that the climax state cannot be reached in mixed forest under the current ecological pressures in general and the lack of sufficient biodiversity in particular. The succession rather terminates at the stage of subdominant diasporic subclimax—a phenomenon which traditional Markov chain models are unable to reproduce. We suggest a formalisation of the logic why the subclimax-to-climax transition does not occur under the above conditions, and this results in a non-Markov version of the traditional model. We show, by solving a non-linear eigenvalue problem and studying the asymptotic behaviour, that the limit vector of state probabilities depends non-trivially on the initial conditions. Convergence to the climax state takes place only for a restricted set of initial vectors representing a sufficient level of biodiversity, while the non-Markov chain absorbs at a subclimax state for other initial conditions. © 2001 Elsevier Science B.V. All rights reserved.

Keywords: Mixed forest; Succession; Non-Markov model; Transition probabilities; Climax; Non-attainability effect

1. Introduction

Markov chain models of succession have long been used to formalise the course of successional

changes in terrestrial vegetation and to produce certain predictions in quantitative form. Publications using this kind of model in ecological studies boomed in the 70s and early 80s (see reviews in Horn, 1975, 1981; Usher, 1979, 1981; Mirkin and Naumova, 1984), after which the boom waned again. Recent applications, however, revived both practical interest in Markov models and theoreti-

* Corresponding author. Tel.: + 7-95-2846047; fax: + 7-95-9531652.

E-mail address: danilal@postman.ru (D.O. Logofet).

cal debate on what these models can really predict in vegetation dynamics (see e.g. Usher, 1992; Acevedo et al., 1995; Li, 1995; Logofet, 1999; Balzter, 2000; Logofet and Lesnaya, 2000).

At the background of sophisticated 'individual-tree' or 'gap' models of forest dynamics (Shugart, 1984), the Markov chain models of forest succession, with their direct correspondence to the given schemes of successional changes and their deliberate omission of any cause-effect mechanisms, may seem to be too simple. However 'simple' is not synonymous with 'bad' or 'inadequate', just as 'dynamics' is not a rigorous synonym of 'succession'. As a straightforward formalisation of the geobotanic knowledge expressed as a succession scheme, the traditional (time-homogeneous) Markov chain model has certain didactic advantages: its inherent mathematical property to converge to a limit probability distribution of states of the chain fits well the classic, Clementsian, paradigm of succession theory, the distribution being usually interpreted as the climax state of vegetation in the ideal course of succession. But this can hardly serve a tool for realistic predictions under conditions of climate change (Logofet, 1999; Logofet and Denisenko, 1999), which requires at least time-inhomogeneous versions of the traditional model (Logofet et al., 1997).

Even with a time-homogeneous Markov chain, the way of climax acquisition depends essentially on whether or not the chain is constructed as an *absorbing* one (see a formal definition below). The very nature of the climax in mixed, coniferous-broad-leaved forest in Central Russia (Section 2) might admit various approaches to climax acquisition in a Markov chain model of succession, and Section 3 illustrates perhaps the simplest one: it treats the absorbing state of the chain as the climax stage of succession among forest types typical for the case study mentioned; any initial distribution of states absorbs eventually in the climax state.

However, geobotanic experts believe that the climax state cannot be reached in mixed forests under the current ecological pressures in general and the lack of sufficient biodiversity in particular (Razumovskii, 1981; Popadyuk et al., 1994; Za-ugolnova, 2000). The succession rather terminates at the stage of subdominant diasporic subclimax—a phenomenon which traditional Markov chain models are unable to reproduce. In Section 4, we suggest a formalisation of the logic why the subclimax-to-climax transition does not occur under the above conditions, and this results in a *non-Markov* version of the traditional model. We analyse further a simplified, low-dimensional version of the original model and reveal its spectrum of asymptotic behaviour, including the climax non-attainability effect, which is qualitatively different from that of traditional Markov chain models of succession.

2. Characteristics of the object to model

The territory under study includes the 'Russkii Les' ('Russian Forest') Pilot Forestry and the neighbouring Prioksko-Terrasnyi Reserve, which are both located 100 km south of Moscow on the left riverside of the Oka River. It is well suited for modelling since successions proceeding under reserve conditions can be contrasted with those under forestry activities.

The territory belongs to the coniferous-broad-leaved forest subzone (Isachenko, 1980). The landscape can be classified into three major categories here, river terraces; upland terraces; and watersheds. The scheme of succession has been developed for the watershed territory. Fig. 1 shows an ideal (in the absence of disturbances) course of successions through forest types after a tillage area was abandoned—a scenario of forest secondary succession typical for the land-use history in the region. The numerals in boxes enumerate the stages of succession, which are specified in this way and supplied with estimates of the average duration times. The latter are obtained from data on the ontogenesis duration for arboreal species and substantiated with materials from observations in the southern part of Moscow Region (Rysin, 1985; Popadyuk et al., 1994; Smirnova et al., 1995).

Natural overgrowing of the tillage area begins with invasion of pioneer tree species represented

mainly by common birch (*Betula pendula* Roth.) and white birch (*Betula pubescens* Ehrh.) mixed with aspen (*Populus tremula* L., stages 1 and 2 in Fig. 1). Under the lucid canopy formed by small-leafed species, there are conditions favourable for establishment of the secondary and climax tree species (*late-successional* species), the species composition being determined primarily by the potential of seed introduction. As seed dispersal occurs over a few hundred meters in the majority of late-successional species (see below), there may develop situations of seed deficiency. For example, a birch forest with spruce undergrowth develops under the presence of common spruce (*Picea abies* (L.) Karst.) seeds and the lack of seeds of other potential dominant species (stage 3); other

types of forest develop by similar mechanisms (stages 4–6).

Forest scientists were the first who paid attention to regularities in the tree species dissemination when observing the natural forest renewal on cutting areas of different sizes (Dekatov, 1936; Molchanov and Gubareva, 1965; Ogievskii, 1966). The range of efficient seed dispersal for the anemochorous (= wind-dispersed) common spruce turned out to cover up to 200 m (Dekatov, 1936; Luk'yanets, 1982). Anemochorous small-leafed species, such as aspen, birch and willow (*Salix* spp.), cannot disperse farther than 1–1.5 km (Lositskii, 1968; Luk'yanets, 1982; Udra, 1990). Hemianemochorous species, such as small-leafed lime (*Tilia cordata* Mill.), Norway maple
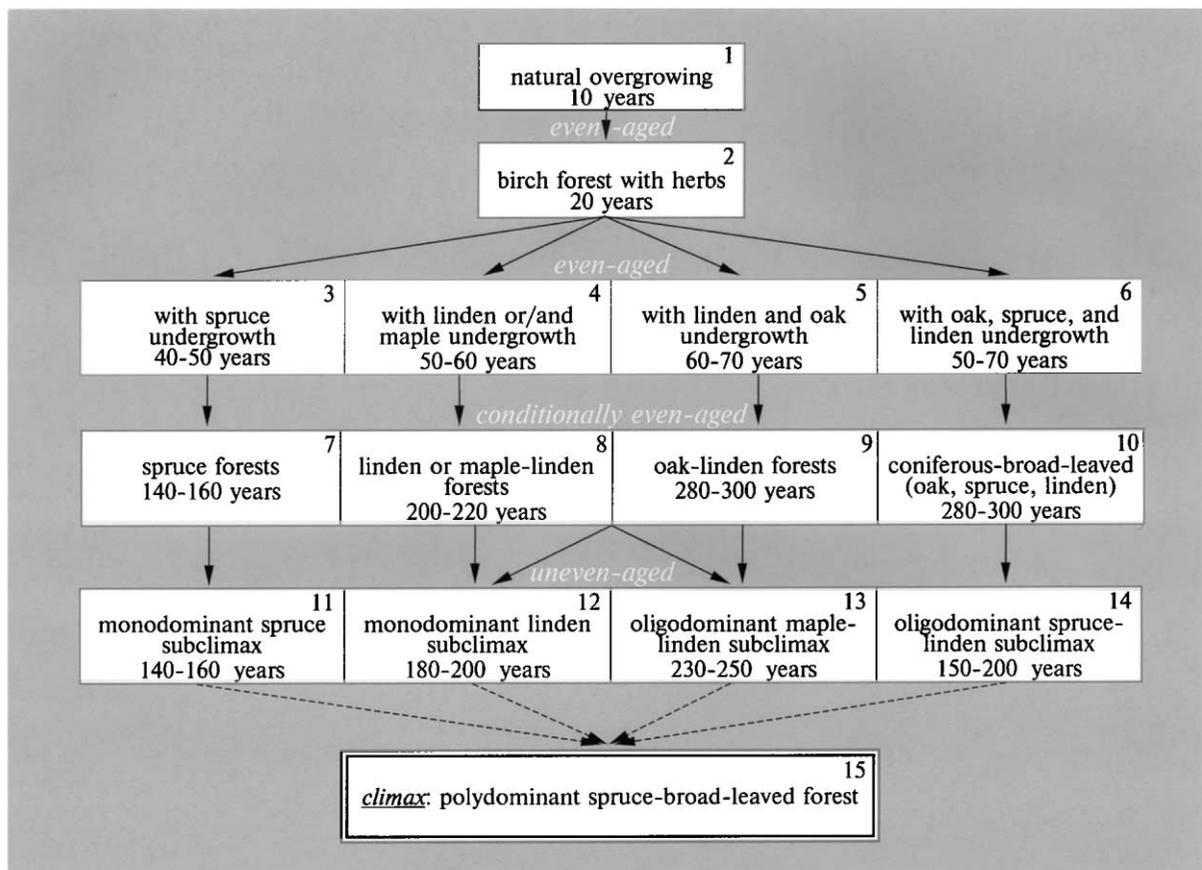

Fig. 1. Ideal course of succession through forest types (after-tillage series) in the Prioksko-Terrasnyi Biosphere Reserve, Moscow Region, Russia.

Table 1
Areas of the main successional types in 'Russkii Les' Pilot Forestry

Successional type	Number	Area (ha)	Relative area (%)
Monodominant types			
Birch forest with spruce undergrowth	3	1279.84	22.9
Birch forest with lime undergrowth	4	1436.07	25.7
Birch forest with oak and lime undergrowth	5	339.06	6.1
Birch forest with oak, lime and spruce undergrowth	6	962.79	17.2
Spruce forest	7	691.38	12.4
Lime forest	8	234.51	4.2
Oligodominant types			
Oak-lime forest	9	236.98	4.2
Spruce-oak-lime forest	10	413.44	7.4
Total		5594.07	100.0

(*Acer platanoides* L.), elm (*Ulmus* spp.) and common ash (*Fraxinus excelsior* L.), with heavy winged seeds, can cover significantly shorter distances, 100–200 m (Udra, 1988). Nuciform fruits of barochorous–zoochorous (= gravity- and animal-dispersed) species, such as English oak (*Quercus robur* L.) and European hazel (*Corylus avellana* L.), fall primarily under the crowns of their maternal trees, yet dissemination within the range of 300–500 m is provided by some birds (mainly by jay *Garrulus glandarius* L., Ridley, 1930; Holodnyi, 1941; Lositskii, 1968; Vladyshevskii, 1980).

The next stage of succession is related to breakdown of the birch stands occurring at the 75–100-year age. After a birch stand breaks down, there is a new stand forming, not so even in the age structure and with a variable set of late-successional tree species (stages 7–10). In a period of time equal to the life span of those tree species, the second (since overgrowing began) generation of tree species breaks down and uneven-aged communities of the subclimax type begin to develop (stages 11–14). The luciphilous oak disappears and the subclimax stand consists of shade-tolerant species only (lime, spruce, maple, etc. in various combinations). When appropriate seeds are lacking, the succession can delay at a subclimax stage indefinitely long. If seeds are introduced in a natural or artificial way, then a climax forest can form (the corresponding transitions to stage 15 are shown by dashed arrows in Fig. 1).

Present views of succession in mixed boreal forest (Korotkov, 1991; Remmert, 1991; Popadyuk et al., 1994; Smirnova et al., 1995; Zaugolnova, 2000) consider the climax stage as a multi-aged, polydominant, spruce-broadleaf forest whose species composition includes all the major tree *dominants* (i.e. those species exerting the most influence on community composition, see Greig-Smith, 1986; Allaby, 1998), namely, spruce, linden, maple, elm, etc.

Application of a GIS-technology (see Appendix D for some detail) enabled estimating the areas of the main successional types in the 'Russkii Les' Pilot Forestry (Table 1). The lack of stages 11–15 in the Forestry, in contrast to the neighbouring Reserve, can be explained by severe anthropogenic transformations. Current forest ecosystems have been forming in the Forestry area after strong anthropogenic disturbances occurred 60–90 years ago. For a completely uneven-aged forest of a subclimax type to develop, much longer time is needed without drastic disturbances (such as cutting, ploughing). In addition to prolonged absence of disturbances, easy introduction of seeds of the zonal dominant tree species is of great importance for reaching the climax (stage 15).

3. Climax as an absorbing state

The traditional formalism for Markov chain models of succession suggests that the states of

the chain are identified with the specified stages of succession and enumerated by natural numbers from 1 to 15, as shown in Fig. 1. The major problem is to estimate the entries of the *transition probability matrix* $P(1) = [p_{ij}(1)]$, where $p_{ij}(1)$ designates the probability that state i changes into state j in one time step (i, $j = 1,2,$ ..., 15). The data in Fig. 1 allow construction of the matrix $P(1)$ by a simple method of p_{ij} estimation (Logofet and Lesnaya, 2000): if m_i is the *average duration* given in the scheme for stage i, then the diagonal entries of $P(1)$ are

$$p_{ii} = 1 - \frac{1}{m_i}, \quad i = 1, 2, \ldots 14; \quad p_{15, 15} = 1; \quad (1)$$

if there is no arrow $i \rightarrow j$ in the scheme for a particular pair of indices $i \neq j$, then $p_{ij}(1) = 0$; if there are $k \geq 1$ arrows $i \rightarrow j$ outgoing from state i, then

$$p_{ij} = \frac{1}{(km_i)}, \quad (2)$$

under assumption that all the transitions from state i are equiprobable. The assumption is not crucial for the method: any a priori knowledge of the ratios among the k values of p_{ij} for $i \neq j$ (which must total to $1/m_i$ due to the stochastic property of matrix $P(1)$) can determine those values in a unique way (Logofet and Lesnaya, 2000).

If the time step is chosen to be $\Delta t = 5$ year (it can be neither too small, nor greater than the shortest average duration among all stages), then the scheme of Fig. 1 suggests the following vectors of m_i-values:

$$\boldsymbol{m}_{\min} = [2\ 4\ 8\ 10\ 12\ 10\ 28\ 40\ 56\ 56\ 28\ 36\ 46\ 30],$$

$$\boldsymbol{m}_{\min} = [2\ 4\ 10\ 12\ 14\ 14\ 32\ 44\ 60\ 60\ 32\ 40\ 50\ 40],$$

with the components corresponding, respectively, to the minimal and maximal values of stage duration. The transition probability matrices $P_{\min}(1)$ and $P_{\max}(1)$ are then easily constructed by formulae (Eqs. (1) and (2)).

Let $x(t)$ denote a stochastic vector whose component $x_i(t)$ shows the probability that the chain is in state i ($i = 1,2,$ ..., 15) after t time steps ($t = 0, 1, 2, \ldots$). Vector $x(t)$ is thus the *state probability vector*. The Markov property results in the well-known linear dynamic equation (see e.g. Roberts, 1976):

$$\boldsymbol{x}(t + 1) = \boldsymbol{x}(t)P(1), \quad t = 0, 1, 2, \ldots, \quad (3)$$

with the general solution

$$\boldsymbol{x}(t) = \boldsymbol{x}(0)P(1)^t, \quad t = 0, 1, 2, \ldots. \quad (4)$$

Given an initial distribution of state probabilities $x(0)$—identified usually with the relative area composition of the corresponding types in the mosaic of vegetation (see Table 1),—formula (4) turns calculation of $x(t)$ into a matter of simple matrix multiplication.

Both the scheme in Fig. 1 and the term $p_{15,15} = 1$ guarantee that state 15 is an *absorbing* state of the chain, i.e. a state which, once entered, is never left again. In contrast, states 1–14 are *transient*, i.e. once left, they are never entered again. Both the theory of finite Markov chains and explicit calculation of the limit vector

$$\boldsymbol{x}(\infty) = \boldsymbol{x}(0)P(\infty), \quad P(\infty) = \lim_{t \to \infty} P(1)^t, \quad (5)$$

for either matrix $P_{\min}(1)$, or $P_{\max}(1)$, indicate that any initial composition $x(0)$ converges asymptotically to $x(\infty) = [0, \ldots, 0, 1]$, i.e. absorption in the climax state.

This trivial prediction follows also from a common-sense view on the succession scheme, but there are non-trivial predictions of how long it takes, on the average, to reach the climax state starting from any transient state i. This kind of prediction relies on the *fundamental matrix*

$$N = (I - Q)^{-1}, \quad (6)$$

which exists for any absorbing Markov chain (Kemeny and Snell, 1960). Here Q is the 14×14 submatrix of $P(1)$ covering transitions among the transient states, $I = \text{diag}\{1, \ldots, 1\}$ is the *identity matrix* of equivalent size. Element n_{ij} of matrix N indicates the expected number of time steps the chain sojourns at state j if started from state i. If we take submatrix Q from $P_{\min}(1)$, then Eq. (6) yields (as integers)

$$N_{\min} = \begin{bmatrix}
2 & 4 & 2 & 3 & 3 & 3 & 7 & 10 & 14 & 14 & 7 & 9 & 11 & 7 \\
0 & 4 & 2 & 3 & 3 & 3 & 7 & 10 & 14 & 14 & 7 & 9 & 11 & 7 \\
0 & 0 & 8 & 0 & 0 & 0 & 28 & 0 & 0 & 0 & 28 & 0 & 0 & 0 \\
0 & 0 & 0 & 10 & 0 & 0 & 0 & 40 & 0 & 0 & 0 & 18 & 23 & 0 \\
0 & 0 & 0 & 0 & 12 & 0 & 0 & 0 & 56 & 0 & 0 & 18 & 23 & 0 \\
0 & 0 & 0 & 0 & 0 & 10 & 0 & 0 & 0 & 56 & 0 & 0 & 0 & 30 \\
0 & 0 & 0 & 0 & 0 & 0 & 28 & 0 & 0 & 0 & 28 & 0 & 0 & 0 \\
0 & 0 & 0 & 0 & 0 & 0 & 0 & 40 & 0 & 0 & 0 & 18 & 23 & 0 \\
0 & 0 & 0 & 0 & 0 & 0 & 0 & 0 & 56 & 0 & 0 & 18 & 23 & 0 \\
0 & 0 & 0 & 0 & 0 & 0 & 0 & 0 & 0 & 56 & 0 & 0 & 0 & 30 \\
0 & 0 & 0 & 0 & 0 & 0 & 0 & 0 & 0 & 0 & 28 & 0 & 0 & 0 \\
0 & 0 & 0 & 0 & 0 & 0 & 0 & 0 & 0 & 0 & 0 & 36 & 0 & 0 \\
0 & 0 & 0 & 0 & 0 & 0 & 0 & 0 & 0 & 0 & 0 & 0 & 46 & 0 \\
0 & 0 & 0 & 0 & 0 & 0 & 0 & 0 & 0 & 0 & 0 & 0 & 0 & 30
\end{bmatrix}$$

The row sums (multiplied by the time step length) now give the estimation (in years) of how long the succession proceeds before reaching the climax stage if started from any earlier stage i:

$$T_{\min} =$$

[480 470 320 455 545 480 280 405 485 430 140 180 2 30 150]^T.

When calculated for matrix $N_{\max}$ (not cited), the estimation yields:

$$T_{\max} =$$

[540 530 370 505 595 570 320 445 525 500 160 200 2 50 200]^T.

So, it would take from 480 to 540 years, on the average, for the ideal course of succession to reach the climax stage from the pioneer one and, respectively, lesser times from the later stages. Although some of these predictions might be regarded trivial by common sense relying on Fig. 1,
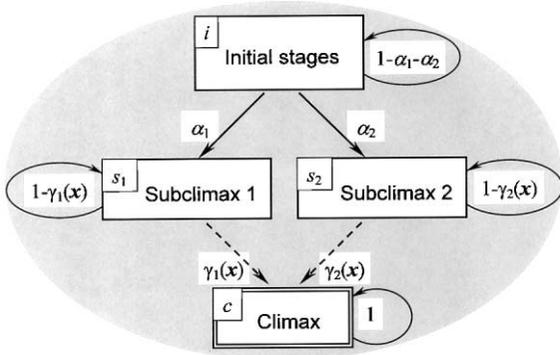

Fig. 2. Aggregated model of forest succession. Inscriptions assigned to arrows designate the corresponding one-step transition probabilities.

like e.g. those for the pathways $3 \rightarrow 7 \rightarrow 11 \rightarrow 15$, 320–370 year, or $6 \rightarrow \ldots \rightarrow 15$, 480–570 year, the predictions are not so obvious for the pathways to climax with alternative transitions, especially if the alternative transitions were not equiprobable.

4. Climax non-attainability

There is a complex, mosaic-layer structure of forest community developing in the course of succession. A completely uneven-aged stand may recover under various numbers of species in the potential flora. In the current conditions, however, the species composition depends drastically on opportunities for seed introduction and for establishment of the young generations of late-successional tree species. There are *successional* (i.e. transient) types dominating nowadays in the forest cover of man-modified territories, while the *terminal* (i.e. climax or subclimax) stages can only develop under prolonged absence of human-induced disturbances. The latter can be observed in reserves, but even in the reserves, the century-old history of land-use has resulted in losses of biological diversity.

Biodiversity losses may delay succession, prevent the establishment of the climax stage and favour diasporic subclimax stages in forest successions through the following 'mechanisms':

- disappearance of some late-successional tree species due to severe anthropogenic pressure on the vegetation cover;
- small ranges of seed dispersal in the crucial species (see above in Section 2), in combination with
- forest fragmentation and the 'island' pattern of forest tracts.

To explore the potential of chain models in modelling the climax non-attainability effect, we aggregate the scheme in Fig. 1 into a simplified, four-state chain as shown in Fig. 2. Under *Subclimax* 1 and *Subclimax* 2 one can mean, for instance, the mixed and deciduous types of forest, respectively. Then the aggregated state i includes all the former stages 1–10, state s_1 consists of the former stages 11 and 14, and state s_2 consists of 12 and 13. The climax state c is an absorbing state
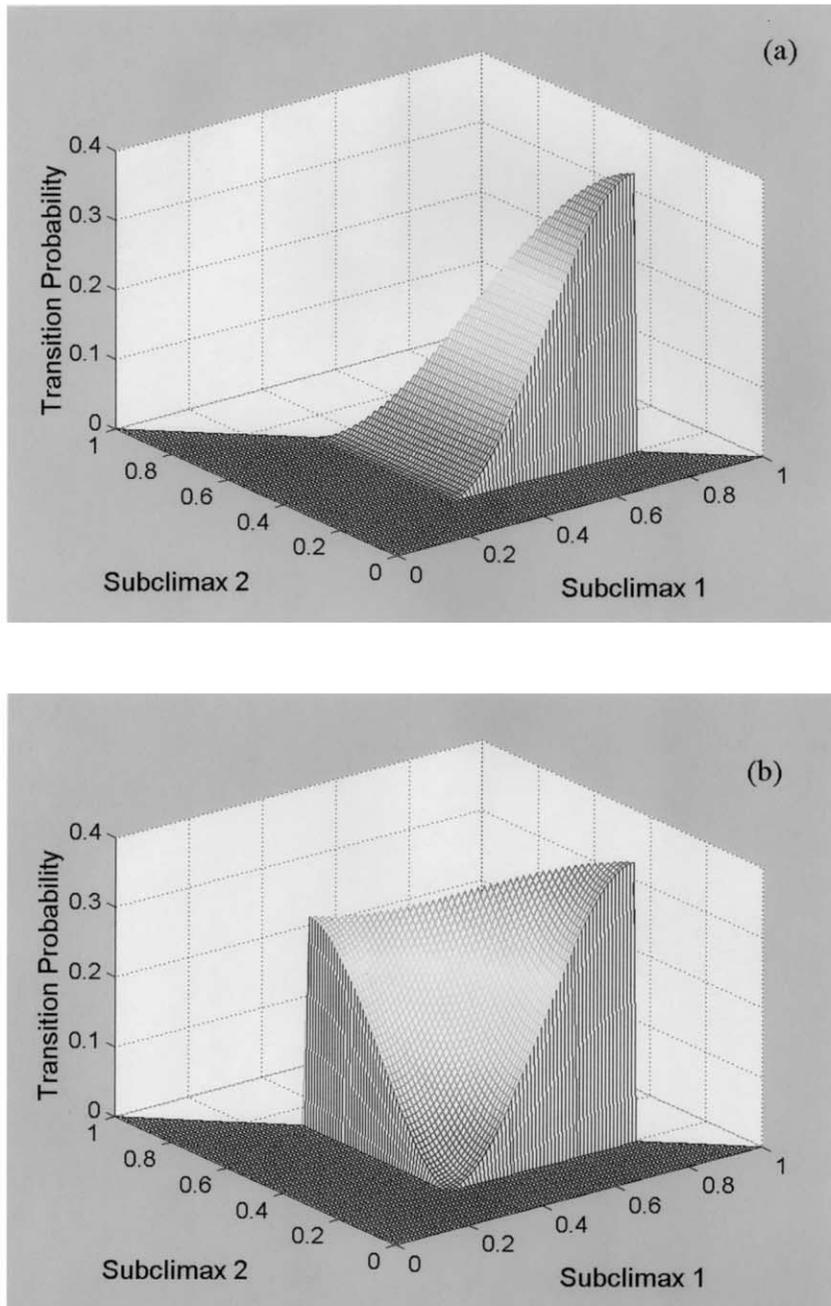
Fig. 3. Subclimax-to-climax transition probabilities as functions (8) of the state probability vector components s_1 and s_2 for particular illustrative values of the threshold parameters $d_1 = 0.3$, $d_2 = 0.2$ and cubic-spline growth of $\gamma_1(s_1)$, $\gamma_2(s_2)$ up to maximal levels $\gamma_1^{max} = 0.4$, $\gamma_2^{max} = 0.3$: (a) $\gamma_1(x)$; (b) $\gamma_1(x) + \gamma_2(x)$.
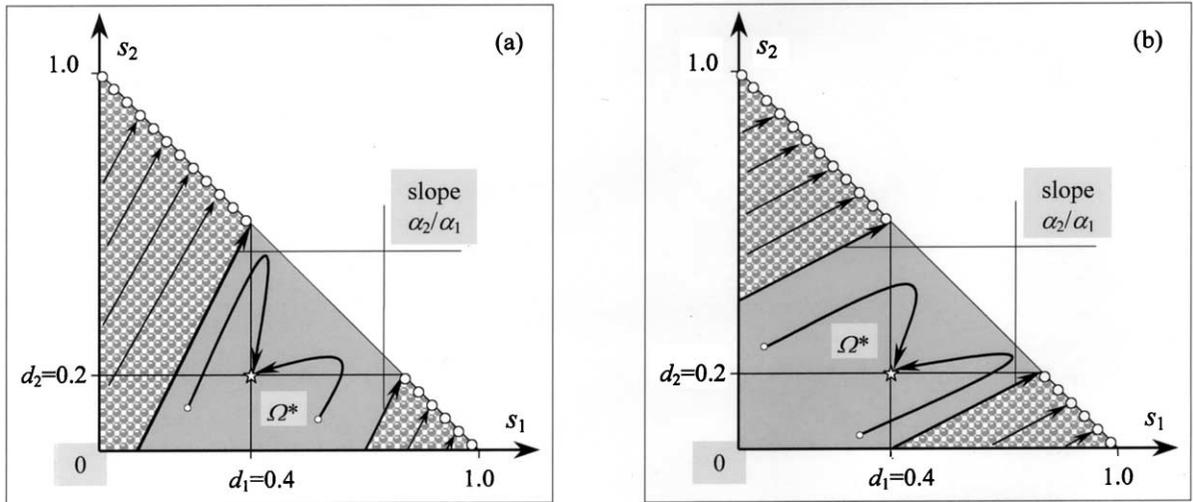
Fig. 4. Patterns of convergence for trajectories of the non-Markov chain model starting in the subspace $\{s_1, s_2, c = 0\}$. The model parameters are the same as in Fig. 3: (a) $\alpha_2/\alpha_1 = 2$; (b) $\alpha_2/\alpha_1 = 1/2$.

as before, and the state probability vector is now represented by four components:

$$x(t) = [i(t), s_1(t), s_2(t), c(t)]. \tag{7}$$

To formalise the logic why the climax stage of forest succession cannot be reached under insufficient biodiversity, we assume biodiversity to be sufficient when the subclimax stages (11–14 in Fig. 1) of succession are all present in the forest. In terms of vector (7), it means that the components $s_1(t)$, $s_2(t)$ should be somehow balanced. We assume furthermore that transition to climax does not occur unless both $s_1(t)$ and $s_2(t)$ are great enough, e.g. exceed some threshold values; if the transition $s_i \to c$ does occur on the time step t, then its probability, $\gamma_i(x)$ ($i = 1, 2$), is greater, the greater is the portion $s_i(t)$ in the state probability vector $x(t)$. In formal terms,

$$\Pr\{s_i \to c\} = \gamma_i(x)$$

$$= \begin{cases} 0 \text{ if } (s_1 \leq d_1) \vee (s_2 \leq d_2), \\ \gamma_i(s_i) \text{ otherwise } (0 < \gamma_i(s_i) \leq \gamma_i^{\max}) \end{cases} \tag{8}$$

with some threshold parameters d_1, d_2 and any scalar, monotone increasing function $\gamma_i(s_i)$, $i = 1$, 2. Since x is a stochastic vector, functions $\gamma_i(x)$ are defined on the simplex $\{s_1 + s_2 \leq 1\}$. It is clearly

seen in Fig. 3 that $\gamma_i(x) = 0$ outside the triangle $\{s_1 \geq d_1, s_2 \geq d_2, s_1 + s_2 \leq 1\}$ and $\gamma_i(x)$ increase monotonically inside it. It makes sense to consider only the cases where $d_1 + d_2 < 1$; otherwise transition to climax is never possible.

According to the scheme in Fig. 2, the transition probability matrix takes on the form $P(x)$

$$= \begin{bmatrix} 1 - \alpha_1 - \alpha_2 & \alpha_1 & \alpha_2 & 0 \\ 0 & 1 - \gamma_1(x) & 0 & \gamma_1(x) \\ 0 & 0 & 1 - \gamma_2(x) & \gamma_2(x) \\ 0 & 0 & 0 & 1 \end{bmatrix} \tag{9}$$

with α_1 and α_2 ($0 < \alpha_i < 1$) estimating transitions from the initial stages of succession to the subclimax ones and with functions $\gamma_i(x)$ as above. Note that state $s_i (i = 1, 2)$ becomes an absorbing one whenever any $\gamma_i(x) = 0$.

Since the transition probabilities now depend non-trivially on the current state vector x, the chain is no longer Markov. The linear Eq. (3) transforms, by substitution of $P(1)$ with $P(x)$, into

$$x(t + 1) = x(t)P(x(t)), \quad t = 0, 1, 2, \ldots, \tag{10}$$

allowing one to find $x(t)$ successively at any time step, starting with any given $x(0)$, yet lacking the

elegant formula (4). Nevertheless, the limit vector $x(\infty)$ can be shown to exist and be calculable as a solution to the non-linear eigenvector problem for the operator (9) (see Appendix A).

The solution determines the asymptotic behaviour in the non-Markov chain model (7)–(10); Fig. 4 shows this behaviour projected onto the (s_1, s_2) plane. There is a region Ω^* in the plane, whose size and slope is determined, in a visible way, by the model parameters d_1, d_2, α_1 and α_2. Initial vectors $x(0) = [i(0), s_1(0), s_2(0), c(0)]$ outside (or on the lateral boundaries of) Ω^* can be proved (Appendix A) to converge to their respective equilibria, each lying on the hypotenuse $s_1 + s_2 = 1 - c(0)$ (shown in Fig. 4 is the case where $c(0) = 0$). Initial vectors inside (or on the hypotenuse boundary of) Ω^* converge asymptotically to the single equilibrium vector

$$x^* = [0, s_1^* = d_1, s_2^* = d_2, c^* = 1 - d_1 - d_2] \qquad (11)$$

which can be interpreted as *partial absorption* at the climax state (this is proved in Appendix A for sufficiently small parameters γ_i^{max}, which is guaranteed by the number of time steps to the climax having the order of $1/\gamma_i^{max}$ and being long enough).

To reach the *subclimax-to-climax* equilibrium (11), the system has originally to possess a certain level of biodiversity expressed in the location of Ω^* in the middle of the simplex $\{s_1 + s_2 \leq 1\}$. Note that parameters α_1 and α_2, the rates of transitions from initial stages, do not affect the final composition of x^* but do determine the pattern of Ω^*.

If interpreted in stability terms, the asymptotic behaviour in the non-Markov model (7)–(10) looks as follows. The *subclimax-to-climax* equilibrium x^* is asymptotically stable globally in the region Ω^*. Each initial vector outside Ω^* converges to its own equilibrium vector x° defined by Eqs. (A.8) and (A.9) and corresponding to absorption in the subclimax states. All these equilibria are locally non-asymptotically stable in the sense that any small perturbation of the initial vector x° generates a limit vector whose deviation from x° is small too. This is guaranteed by the linear mode (Eqs. (A.8) and (A.9)) in which the limit vector depends on the initial one.

Note that the findings above do not depend on the particular form of functions $\gamma_i(x)$, nor on parameters γ_1^{max}, γ_2^{max} (except for them being sufficiently small). The latter may, however, influence time estimations. The average time it takes for total absorption in the subclimax states can be calculated by the technique known for absorbing Markov chains. The 1×1 submatrix $Q = [1 - \alpha_1 - \alpha_2]$ of the transition probability matrix (9) yields the fundamental 'matrix' (Eq. (6)) $N = 1/(\alpha_1 + \alpha_2)$, which gives the average number of time steps needed to reach an absorbing subclimax state. Although we analyse the aggregated chain aiming at its qualitative asymptotic behaviour, its parameters may be given quantitative estimates consistent with the way of aggregation (Appendix B).

As regards absorption in the climax state, the process is essentially non-Markov, hence the Markovian technique is no longer applicable. If, however, we majorize the non-zero transition probabilities $\gamma_i(x)$ with their constant maximal values γ_i^{max}, then the resulting chain will be apparently Markov and absorbing faster than the non-Markov chain. It means that the fundamental matrix of the majorizing chain (see Appendix C) can be regarded as a lower estimate for the average times before climax absorption in the non-Markov chain. For the particular estimates of α_1, α_2, γ_1^{max}, γ_2^{max} derived in Appendix B, formula (C.2) gives

$$N_{min} = \begin{bmatrix} 61 & 16 & 19 \\ 0 & 29 & 0 \\ 0 & 0 & 41 \end{bmatrix},$$

whereby $T_{min} = [96 \ 29 \ 41]^T \times 5$ year, which is quite consistent with the estimates presented in Section 3.

Whether the threshold parameters d_1 and d_2 are amenable to estimation is discussed below.

5. Discussion

While an absorbing Markov chain model of succession has no other fate than to absorb at the absorbing state(s) interpreted usually as the cli-

max stage(s) of succession, the proposed non-Markov chain has essentially different pattern of asymptotic behaviour. In particular, the limit vector of state probabilities now depends non-trivially on the initial conditions: convergence to the climax state takes place only for a restricted set of initial vectors representing a sufficient level of biodiversity in the mosaic of forest types, while the non-Markov chain absorbs in a subclimax state for other initial conditions. No standard analytical method exists for estimation of the average time it would take to reach the climax state in the non-Markov version, but the Markovian technique can produce, as we see in the previous section, the minimal estimates for that time. A series of direct Monte-Carlo experiments might give an idea of how close those estimates could be to the 'actual' value.

As regards quantitative estimation of the threshold parameters d_1 and d_2 in the transition probabilities to the climax stage, the task may seem unfeasible since their original meanings, which resulted in formula (8) are pure hypothetical. The analysis, however, has revealed that d_1 and d_2 determine the *subclimax-to-climax* equilibrium composition in the proposed non-Markov model (see Eq. (11) and Fig. 4), thus revealing an opportunity to solve the estimation problem through model calibration versus real or/and theoretical data on the equilibrium composition. To extract this kind of data from a mosaic of forest types, an expert should be mastered with quantitative criteria for classifying a forest type as a subclimax or climax stage of succession. These would require further quantification for the level of biodiversity that is inherent in the geobotanic concept of climax as polydominant mixed forest. Such quantification, when based on a deeper insight into the species composition of the 'polydominant forest' and into those of the oligodominant subclimax stages, might be achieved through application of GIS-technologies in forest reserves at sufficiently fine-grain scales of resolution.

The Markov- and non-Markov chain models considered do not explicitly include any spatial dimension. Meanwhile, the rationale for climax non-attainability in stressed forest (Section 4) does include the spatial aspects such as small ranges of seed dispersal and forest fragmentation. The corresponding logical complication of our models might be implemented in the framework of cellular automata models for vegetation dynamics on a grid of 'cells' in which the state of a cell changes also as a function of the state in its closest neighbours (Balzter et al., 1998). In a proper spatial scale related to that of seed dispersal, this would result in a *spatio-temporal Markov chain* (*ibidem*), for which the question would then arise whether any Markov setting be sufficient to reproduce the climax non-attainability effect or a kind of non-Markov formulation be necessary.

An alternative approach to climax acquisition in a Markov chain model might rely on a balance between disturbance and regeneration processes, which would perhaps be closer to the modern paradigm of succession in mixed forests (Korotkov, 1991). This would require modification of the former (idealised) conceptual scheme by introducing some reverse transitions to the earlier stages of succession, which would result in cycles of regeneration succession, hence in a chain that would no longer be absorbing. We have deliberately chosen not to proceed along this approach in the present paper since the task was to study a non-Markov potential in reproducing the climax non-attainability effect. Meanwhile, further efforts in GIS technologies might help estimating the rate of natural or man-made disturbances in the area, hence opening a gate for introducing scenarios of forest management into chain models of forest succession.

6. Conclusion

While a traditional Markov chain model predicts inevitable absorption in the climax state, its proposed non-Markov modification has fundamentally distinct asymptotic properties and is capable of reproducing the climax non-attainability effect. The non-climax transition parameters of this aggregated model can be derived from the original, disaggregated chain in a straightforward way. Unfortunately, the threshold parameters of the transition-to-climax probabilities cannot be

estimated in a similar way since they are precisely responsible for the dissimilarity between the Markov and non-Markov chains considered. Further progress in developing a GIS representation of the object under study might suggest some guidelines for making the estimation problem solvable, which would certainly improve the descriptive and predicting potentials of the non-Markov chain models.

Acknowledgements

Appendix A

The eigenvector problem for the (unitary eigenvalue of) non-linear operator (9) is to find a vector $x° = [i°, s_1°, s_2°, c°]$ such that

$$x° = x°P(x°), \quad x° \geq 0, \left\| x° \right\|_\Sigma = 1. \quad (A.1)$$

By Eq. (9) the problem reduces to the following system of non-linear equations:

$$\begin{cases} (1 - \alpha_1 - \alpha_2)i° & = i° \\ \alpha_1 i° + [1 - \gamma_1(x°)]s_1° & = s_1°, \\ \alpha_2 i° + [1 - \gamma_2(x°)]s_2° & = s_2°, \\ \gamma_1(x°)s_1° \quad \gamma_2(x°)s_2° + c° & = c°, \end{cases} \quad (A.2)$$

which is equivalent to

$$\begin{cases} i° & = 0, \\ \gamma_1(x°) & = 0, \\ \gamma_2(x°) & = 0, \\ c° & = c°, \end{cases} \quad (A.3)$$

System (A.3) looks indefinite due to the last equation admitting any value of $c°$, $0 \leq c° \leq 1$,

but it becomes definite with the stochasticity condition $\|x°\|_\Sigma = 1$. Let, for definiteness, $d_1 \geq d_2$ $(d_1 + d_2 < 1)$. With due regard to (8), it can be shown that system (A.3) has a unique solution

$$x^* = [0, s_1^* = d_1, s_2^* = d_2, c^* = 1 - d_1 - d_2] \quad (A.4)$$

and a continuum of solutions of the form:
$$x_1° = [0, s_1° \leq d_1, s_2° = 1 - c° - s_1°, c°],$$
$$0 \leq c° \leq 1, \quad (A.5.1)$$

or

$$x_2° = [0, s_1° = 1 - c° - s_2°, s_2° \leq d_2, c°],$$
$$0 \leq c° \leq 1. \quad (A.5.2)$$

It follows from (A.3) that neither particular form of functions $\gamma_i(x)$, nor particular values of parameters $\gamma_1^{max}, \gamma_2^{max}$ are crucial to the solution, but only the ranges where $\gamma_i(x)$ remain zero.

To understand the asymptotic behaviour in the non-Markov chain model (7)–(10), we consider the projection of its 4-D state space onto the 2-D simplex

$$\{(s_1, s_2): s_1 \geq 0, s_2 \geq 0, s_1 + s_2 \leq 1 - c(0)\}. \quad (A.6)$$

Fig. 4 shows this projection for $c(0) = 0$; if $0 < c(0) < d_1 + d_2 < 1$, the picture is the same, with the hypotenuse $s_1 + s_2 = 1 - c(0)$ shifted correspondingly inward. Cases with $c(0) \geq d_1 + d_2$ make apparently no modelling sense.

When both of $\gamma_i(x)$ $(i = 1, 2)$ are zero, the transition matrix (9) reduces to

$$P_0 = \begin{bmatrix} 1 - \alpha_1 - \alpha_2 & \alpha_1 & \alpha_2 & 0 \\ 0 & 1 & 0 & 0 \\ 0 & 0 & 1 & 0 \\ 0 & 0 & 0 & 1 \end{bmatrix}. \quad (A.7)$$

The projection of the vector increment of $x(t)$, by virtue of Eq. (10), is thereafter sloped to abscissa at α_2/α_1, hence parallel to the lateral boundaries of the region Ω^*. It means that if $x(0)$ lies outside (or on a lateral boundary of) Ω^*, then the chain (7)–(10) is governed by transition matrix (A.7) and is thus a Markov chain, with the limit state vector

$$x(\infty) = x(0)P_0(\infty), \qquad (A.8)$$

where

$$P_0(\infty) = \lim_{t \to \infty}(P_0)^t$$

$$\begin{bmatrix} 0 & \alpha_1/(\alpha_1 + \alpha_2) & \alpha_2/(\alpha_1 + \alpha_2) & 0 \\ 0 & 1 & 0 & 0 \\ 0 & 0 & 1 & 0 \\ 0 & 0 & 0 & 1 \end{bmatrix}$$

$$(A.9)$$

It follows that the 2-D increment from $x(0)$ to $x(\infty)$ also has slope α_2/α_1, hence the trajectories starting outside (or on the lateral boundaries of) Ω^* tend to their respective equilibria as shown in Fig. 4. Those equilibria represent the eigenvector solutions given either by Eq. (A.5.1) or Eq. (A.5.2).

If a trajectory starts outside the triangle $\{s_1 \geq d_1, \ s_2 \geq d_2, \ s_1 + s_2 \leq 1 - c(0)\}$, but still inside Ω^*, the same argument as above makes the trajectory to move parallel with the lateral boundaries until it gets into the triangle in some t_Δ time steps. If $x(t)$ belongs to the triangle, then operator $P(x)$ (9) with non-zero $\gamma_i(x)$ still leaves $x(t+1)$ within the triangle when the parameters $\gamma_i^{\max}$ are small enough. It means that the sequence $\{(s_1(t), s_2(t)) | t = t_\Delta + \tau, \ \tau = 0, 1, 2, \ldots\}$ is at least (component-wise) bounded from below by (d_1, d_2). Furthermore, the sequence is (component-wise) monotone decreasing for great enough t since the increment

$$s_j(t+1) - s_j(t) = i(t)\alpha_j - s_j(t)\gamma_j(x(t)), \quad j = 1, 2,$$

with $i(t)$ vanishing geometrically at rate $(1 - \alpha_1 - \alpha_2)$, becomes negative when t is large enough. Any monotone, bounded sequence is well-known to have a unique limit, and passage to the limit in Eq. (10) constrains the limit to be an eigenvector of the non-linear operator $P(x)$ with eigenvalue 1. This eigenvector is apparently given by expression (A.4).

Thus, any trajectory starting within Ω^* converges eventually to the unique equilibrium (A.4), which is shown in Fig. 4 (bending trajectories, which are actually piece-wise smooth due to the discrete time, are pictured smooth for better visibility).

Appendix B

The first row of matrix $N_{\min}$ (and that of $N_{\max}$) for the 15-state chain gives an estimate, consistent with the way of aggregation, for the average number of time steps the aggregated chain stays in state i before it changes:

$$2 + 4 + 25.5 + 29.5 = 61$$

$$(2 + 4 + 29 + 32.5 = 67.5).$$

It means that $\alpha_1 + \alpha_2 = 1/61$ (1/67.5). As the pathways $3 \to 7 \to 11$ and $6 \to 10 \to 14$ are, on the average, faster than $4 \to 8 \to 12/13$ and $5 \to 9 \to 12/13$, the transition probabilities α_1 and α_2 should not be equal. Rather $\alpha_1{:}\alpha_2 = 29.5{:}25.5 \approx 1.16$ (32.5{:}29 $\approx$ 1.12), so that

$$\alpha_1 = 0.0088 \ (0.0078), \qquad \alpha_2 = 0.0076 \ (0.0070).$$

The maximal rate of transition to climax is apparently related to the minimal duration of the corresponding subclimax stage, so that (with $\Delta t = 5$ years) we have

$$\gamma_1^{\max} = \frac{1}{29}; \qquad \gamma_2^{\max} = \frac{1}{41}.$$

Appendix C

In a Markov chain with transition matrix (9) and $\gamma_i(x) = \gamma_i^{\max}$ everywhere, the states i, s_1, s_2 are transient and state c is absorbing. The submatrix Q is formed by the first three rows and the fundamental matrix is therefore

$$N = \left[I - \begin{bmatrix} 1 - \alpha_1 - \alpha_2 & \alpha_1 & \alpha_2 \\ 0 & 1 - \gamma_1^{\max} & 0 \\ 0 & 0 & 1 - \gamma_2^{\max} \end{bmatrix} \right]^{-1}$$

$$= \begin{bmatrix} \alpha_1 + \alpha_2 & -\alpha_1 & -\alpha_2 \\ 0 & \gamma_1^{\max} & 0 \\ 0 & 0 & \gamma_2^{\max} \end{bmatrix}^{-1}. \qquad (C.1)$$

Direct calculation of the inverse matrix yields

$$N =$$

$$\begin{bmatrix} 1/(\alpha_1 + \alpha_2) & \alpha_1/(\alpha_1 + \alpha_2)/\gamma_1^{\max} & \alpha_2/(\alpha_1 + \alpha_2)/\gamma_2^{\max} \\ 0 & 1/\gamma_1^{\max} & 0 \\ 0 & 0 & 1/\gamma_2^{\max} \end{bmatrix}^{-1}.$$

$$(C.2)$$

Appendix D

The cartographic database for 'Russkii Les' Pilot Forestry and Prioksko-Terrasnyi Reserve has been developed by means of TopoL®, a universal software tool (manufactured by HELP SERVICE, Czech Republic) to create geo-information systems. TopoL® enables one to work both with raster data and with cartographic vector data, associating the data with semantic information not only locally but also as external databases (Greshnov and Starostenko, 1999; Starostenko, 2000). Cartographical materials are all presented in the uniform system of Gauss–Kruger coordinates. Topographic maps of the scale 1:10000 provide the cartographic basis (the raster layer), and the vector layer with forest strata boundaries (at the same scale) is referred to the basis. Forest maps are correspondingly related with an accuracy of 10–20 m (Starostenko, D.A., personal communication). Each polygon (forest stratum) has an associated external database with characteristics of the forest ecosystem state, including data on the tree, undergrowth, and underwood layers and the grass cover. The databases were compiled of the 1991 forest inventory data and complemented with data from geobotanic field studies.

References

Acevedo, M.F., Urban, D.L., Ablan, M., 1995. Transition and gap models in forest dynamics. Ecol. Appl. 5, 1040–1055.

Allaby, M., 1998. A Dictionary of Ecology, second ed. Oxford University Press, Oxford, New York, p. 440.

Balzter, H., 2000. Markov chain models for vegetation dynamics. Ecol. Model. 126, 139–154.

Balzter, H., Braun, P.W., Kohler, W., 1998. Cellular automata models for vegetation dynamics. Ecol. Model. 107, 113–125.

Dekatov, N.E., 1936. Simplest Measures to Renew Forest after Final Felling. Goslestekhizdat, Moscow, p. 112 in Russian.

Greig-Smith, P., 1986. Chaos or order—organization. In: Kikkawa, J., Anderson, D.J. (Eds.), Community Ecology: Pattern and Process. Blackwell Scientific, Melbourne, pp. 19–29.

Greshnov, S.P., Starostenko, D.A., 1999. Problems of GIS applications in forestry. GIS-Assotsiatsiya Infromatsionnyi Byulleten 1 (18), 20–21 in Russian.

Holodnyi, N.G., 1941. On oak dissemination under wild conditions. Botanicheskii Zhurnal (Bot. J.) 26 (2-3), 139–147 in Russian.

Horn, H.S., 1975. Markovian properties of forest successions. In: Cody, M.L., Diamond, J.M. (Eds.), Ecology and Evolution of Communities. Belknap Press, Cambridge, pp. 196–211.

Horn, H.S., 1981. Succession. In: May, R.M. (Ed.), Theoretical Ecology: Principles and Applications. Blackwell Scientific, Oxford, pp. 253–271.

Author, A., 1980. In: Isachenko, T.I. (Ed.), Vegetation in the European part of the USSR. Nauka, Leningrad, p. 426 in Russian.

Kemeny, J.G., Snell, J.L., 1960. Finite Markov Chains. Van Nostrand, Princeton, NJ, p. 210.

Korotkov, V.N., 1991. A new paradigm in forest ecology. Biologicheskie nauki (Biol. Sci.) 8, 7–19 in Russian.

Li, B.-L., 1995. Stability analysis of a nonhomogeneous Markovian landscape model. Ecol. Model. 82, 247–256.

Logofet, D.O., 1999. Successional dynamics of vegetation: classical concepts and contemporary models. In: Shilov, I.A. (Ed.), Ecology in Russia at the Turn of the 21st Century, vol. 1, Nauchnyi Mir, Moscow, pp. 70–98, 297–317.

Logofet, D.O., Denisenko, E.A., 1999. Principles of modelling vegetation dynamics with regard to climate changes. Zhurnal Obschei Biologii (J. Gen. Biol.) 60, 527–542 in Russian, with English summary.

Logofet, D.O., Lesnaya, E.V., 2000. The mathematics of Markov models: what Markov chains can really predict in forest successions. Ecol. Model. 126, 285–298.

Logofet, D.O., Denisenko, E.A., Golubyatnikov, L.L., 1997. Inhomogeneous Markov models for succession of plant communities: new perspectives of an old paradigm. Biol. Bull. 24, 506–514.

Lositskii, K.B., 1968. Regeneration of Oakeries. Selkhozizdat, Moscow, p. 359 in Russian.

Luk'yanets, A.I., 1982. Dispersal of arboreal plant seeds through industrial hillocks in Ural. Ekologiya (Ecology) 2, 80–83 in Russian.

Mirkin, B.M., Naumova, L.G., 1984. On the successions in plant communities. Ekologiya (Ecology) 6, 3–11 in Russian.

Molchanov, A.A., Gubareva, V.A., 1965. Oak Growth and Formation on Slashes in Forest-Steppe. Nauka, Moscow, p. 255 in Russian.

Ogievskii, V.D., 1966. Selected Works. Lesnaya Promyshlennost, Moscow, p. 356 in Russian.

Popadyuk, R.V., Chistyakova, A.A., Chumachenko, S.I., Evstigneev, O.I., Zaugol'nova, L.B., Istomina, I.I., Kiseleva, L.L., Kostyaev, S.A., Smirnova, O.V., Toporova, N.A., Frantsuzov, A.V., Hanina, L.G., Chernov, N.I., Yanitskaya, T.O., 1994. East-European Broad-leafed Forests. Nauka, Moscow, p. 364 in Russian.

Razumovskii, S.M., 1981. Regularities in Biocenosis Dynamics. Nauka, Moscow, p. 232 in Russian.

Remmert, H. (Ed.), 1991. The Mosaic-Cycle Concept of Ecosystems. Springer, Berlin, p. 168.

Ridley, H.N., 1930. The Dispersal of Plants Throughout the World. Reeve, London, p. 744.

Roberts, F.S., 1976. Discrete Mathematical Models with Applications to Social, Biological and Environmental Problems. Prentice-Hall, Englewood Cliffs, NJ, p. 559.

Rysin, L.P. (Ed.), 1985. Forests Near Moscow. Nauka, Moscow, p. 280 in Russian.

Shugart, H.H., 1984. A Theory of Forest Dynamics. Springer, New York.

Smirnova, O.V., Popadyuk, R.V., Evstigneev, O.I., Minaeva, T.Y., Shaposhnikov, E.S., Morozov, A.S., Yanitskaya, T.O., Kuznetsova, T.V., Ripa, S.I., Samokhina, T.Y., Romanovskii, A.M., Komarov, A.S., 1995. Current State of Coniferous-Broad-Leaved-Forest in Russia and Ukraine: Historical Development, Biodiversity, Dynamics. Preprint.

Pushchino Research Center, Russian Academy of Sciences, Pushchino, p. 76.

Starostenko, D.A., 2000. Geoinformation technologies in the field of forestry. GIS-Assotsiatsiya, Infromatsionnyi Byulleten, 2 (24), 12–13, 23, in Russian.

Udra, I.F., 1988. Dispersal of Plants and the Issues of Paleo- and Biogeography. Naukova Dumka, Kiev, p. 197 in Russian.

Udra, I.F., 1990. Dispersal and migrations of arboreal plants in the temperate zone of Eurasia. Synopsis of Doctoral (Biological Sciences) Thesis, Central Botanical Garden, Russian Academy of Sciences, Moscow, p. 38, in Russian.

Usher, M.B., 1979. Markovian approaches to ecological succession. J. Anim. Ecol. 48, 413–426.

Usher, M.B., 1981. Modelling ecological succession, with particular reference to Markovian models. Vegetatio 46, 11–18.

Usher, M.B., 1992. Statistical models of succession. In: Glenn-Levin, D.C., Peet, R.K., Veblen, T.T. (Eds.), Plant Succession: Theory and Prediction. Chapman & Hall, London, pp. 215–248.

Vladyshevskii, D.V., 1980. Foraging activity of forest birds and animals and its biogeocenotic role. Synopsis of Doctoral Thesis (Biological Sciences). Forest and Wood Institute, Siberian Branch of the Russian Academy of Sciences, Krasnoyarsk, p. 38, in Russian.

Author, A., 2000. In: Zaugolnova, L.B. (Ed.), Estimation and Conservation of Forest Cover Biodiversity in Reserves of the European Russia. Nauchnyi Mir, Moscow, p. 196 in Russian.